New roles for Nanos in neural cell fate determination revealed by studies in a cnidarian

Justyna Kanska and Uri Frank*

School of Natural Sciences and Regenerative Medicine Institute (REMEDI), National University of Ireland, Galway, Ireland

*Author for correspondence (uri.frank@nuigalway.ie)

Accepted 15 April 2013
Journal of Cell Science 126, 3192–3203

doi: 10.1242/jcs.127233

Summary

Nanos is a pan-metazoan germline marker, important for germ cell development and maintenance. In flies, Nanos also acts in posterior and neural development, but these functions have not been demonstrated experimentally in other animals. Using the cnidarian *Hydractinia* we have uncovered novel roles for Nanos in neural cell fate determination. Ectopic expression of *Nanos2* increased the numbers of embryonic stinging cell progenitors, but decreased the numbers of neurons. Downregulation of *Nanos2* had the opposite effect. Furthermore, Nanos2 blocked maturation of committed, post-mitotic nematoblasts. Hence, Nanos2 acts as a switch between two differentiation pathways, increasing the numbers of nematoblasts at the expense of neuroblasts, but preventing nematocyte maturation. *Nanos2* ectopic expression also caused patterning defects, but these were not associated with deregulation of Wnt signaling, showing that the basic anterior-posterior polarity remained intact, and suggesting that numerical imbalance between nematocytes and neurons might have caused these defects, affecting axial patterning only indirectly. We propose that the functions of Nanos in germ cells and in neural development are evolutionarily conserved, but its role in posterior patterning is an insect or arthropod innovation.

Key words: Hydrozoa, Invertebrate, Differentiation, Stem cells, Neurogenesis, Nematogenesis

Introduction

Nanos is a Zn-finger domain, RNA binding protein acting as a translational repressor. It is known to act in concert with its canonical partner Pumilio. Together, these proteins repress translation of their target genes. Nanos was first described as a posterior marker in *Drosophila* (Lehmann and Nüsslein-Volhard, 1991) and subsequent studies established three main roles for Nanos: first, it is necessary for fly posterior patterning by inhibiting *hunchback* translation. Second, it is crucial for germ cell development, where it mediates self-renewal of germ stem cells, their migration to the gonads, and suppresses somatic fate and premature differentiation (Hayashi et al., 2004). Finally, Nanos fulfils some functions in the nervous system of *Drosophila* (Ye et al., 2004; Brechbiel and Gavis, 2008). *Nanos* expression patterns in various animals are consistent with these functions.

The first identified role of Nanos, posterior patterning, has only been demonstrated experimentally in insects (Schmitt-Engel et al., 2012). The role of Nanos in germ cells, in contrast, seems to be evolutionarily conserved (Mochizuki et al., 2000; Shen and Xie, 2010) and is well documented in a variety of animal species. Using *Nanos* as a germline marker has been common practice even in the absence of functional studies in non-model organisms (Ewen-Campen et al., 2010; Juliano et al., 2010; Wu et al., 2011). Lastly, the function of Nanos in the nervous system is by far the least well studied. Work done in *Drosophila* has shown that Nanos is required for dendrite morphogenesis (Ye et al., 2004; Brechbiel and Gavis, 2008) through an unclear mechanism. In the mouse, *Nanos1* is expressed in the central nervous system, but its function is unidentified (Haraguchi et al., 2003). A role for Nanos in other animals' nervous systems is unknown.

We aimed at studying the role of Nanos in neural development in a member of a basal metazoan phylum, the Cnidaria. Our rationale for conducting this study was twofold: first, cnidarian morphological simplicity enables investigating the role of a potentially important gene in neural development at a cellular resolution *in vivo*. Second, the pivotal phylogenetic position of cnidarians at the base of the Metazoa could provide insight into the early evolution and ancient role of Nanos.

The phylum Cnidaria includes sea anemones, corals, jellyfishes and hydroids. Members of this group display a relatively simple body plan with few cell types that include epithelial, muscle, gland/secretory, neural and stem cells. Some cnidarians are quite well established as model organisms (Putnam et al., 2007; Chapman et al., 2010; Plickert et al., 2012). *Hydractinia echinata* (Fig. 1) is a common cnidarian representative in the European North Atlantic. Throughout the animal's life cycle, a population of stem cells, called interstitial cells, or i-cells for short, continuously provides progenitors to all somatic and germ cell lineages. *Hydractinia* reproduces sexually on a daily basis, has a short and accessible embryonic development, and is amenable to gene expression analysis and manipulation.

The cnidarian nervous system is of particular interest because it is continuously being renewed in the adult animals and because the molecular mechanisms that specify neurons are, at least in part, well conserved with higher animals (Galliot et al., 2009). The main defining feature of cnidarians is a specific sensory/effector cell type, the stinging cell, or nematocyte (also known as cnidocyte). These chemo/mechanosensory cells include a specialized post-Golgi capsule, called nematocyst (cnida). Nematocysts can explosively discharge upon mechanical/chemical stimulation, extruding a barbed tubule and delivering a venom cocktail into prey and predator tissues.

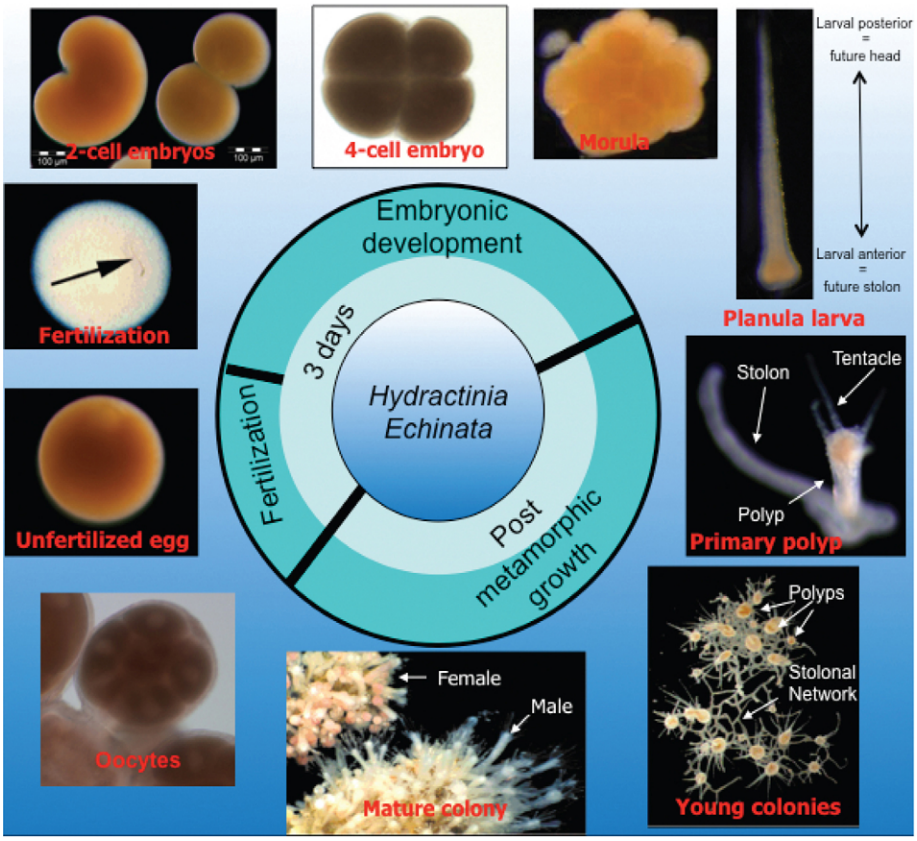

Fig. 1. The life cycle and colony structure of *Hydractinia*.

Using gain and loss of function experiments we show that *Hydractinia* Nanos2 controls nematogenesis at different stages from specification through proliferation to maturation.

Results

Obtaining and analyzing gene sequences

Searching EST databases (Soza-Ried et al., 2010) (and an unpublished 454 library) we identified two cDNA fragments with high sequence similarity to cnidarian and bilaterian *Nanos* genes. The complete coding sequences were obtained by RACE PCR. The genes were named *Hydractinia echinata Nanos1* and *Nanos2*, hereafter *Nanos1* and *Nanos2*, respectively. Two *Nanos* genes were also identified in other cnidarians by others. A Nanos phylogeny has been generated previously (Extavour et al., 2005), suggesting that the two cnidarian *Nanos* genes are a result of a lineage specific duplication. We have repeated this analysis, including also the *Hydractinia* sequences, and our phylogeny is consistent with the data of Extavour et al. (supplementary material Fig. S1).

A single *Hydractinia Pumilio* gene sequence was obtained from the draft assembly of the *Hydractinia* genome (The *Hydractinia* Genome Consortium) and named *Hydractinia echinata Pumilio*, hereafter *Pumilio*. Additional *Nanos* or *Pumilio* sequences were neither identified in the *Hydractinia* EST database or genome draft, nor in other cnidarians genomic and transcriptomic databases, suggesting that cnidarian genomes encode 2 *Nanos* and 1 *Pumilio* genes.

Expression patterns in normal animals

We initially performed *in situ* hybridization to study the normal expression patterns of *Nanos2, Nanos1* and *Pumilio*. Zygotic transcription in *Hydractinia* commences at the morula/gastrula stage (Plickert et al., 2006). *Nanos2* was a maternal transcript, asymmetrically deposited in the prospective oral pole of the embryo and in a Nuage-like deposition around the nuclei of early cleavage stages (Fig. 2A,B). A similar expression has been observed in the hydrozoan *Clytia* (Leclère et al., 2012). Polar bodies are given off at this pole of cnidarian oocytes (Freeman, 1981). This is also the pole where β-catenin is stabilized and the blastopore is formed in species with polar gastrulation (Wikramanayake et al., 2003). Later on this pole develops into the larval posterior end (Plickert et al., 2006). However, following metamorphosis the larval posterior end develops into the adult oral pole of the polyp (also referred to as head; Fig. 1).

Following gastrulation, *Nanos2* was expressed in developing stinging cells (nematocytes; Fig. 2C). Hydrozoan nematocytes and their progenitors, nematoblasts, can be identified morphologically by two ways: first, as nematoblasts proliferate after becoming committed they form characteristic nests or clusters (Lindgens et al., 2004); second, postmitotic nematoblasts or early maturing nematocytes are migratory and can be identified by the developing nematocyst capsule in their cytoplasm.

In the gastrula, at 24 hours post fertilization (hpf) and in the planula larva (48 hpf), *Nanos2* was expressed in two stages of nematocyte differentiation: first, in clusters of dividing nematoblasts in the endodermal cell mass; second, in maturing nematocytes in both the endoderm and in the ectoderm (Fig. 2C). Note that in cnidarian literature ‘ectoderm’ and ‘endoderm’ usually refer to the outer and inner cell layers (also known as epidermis and gastrodermis), respectively, regardless of their embryonic origin. In hydroids like *Hydractinia*, for example, i-cells, neurons and

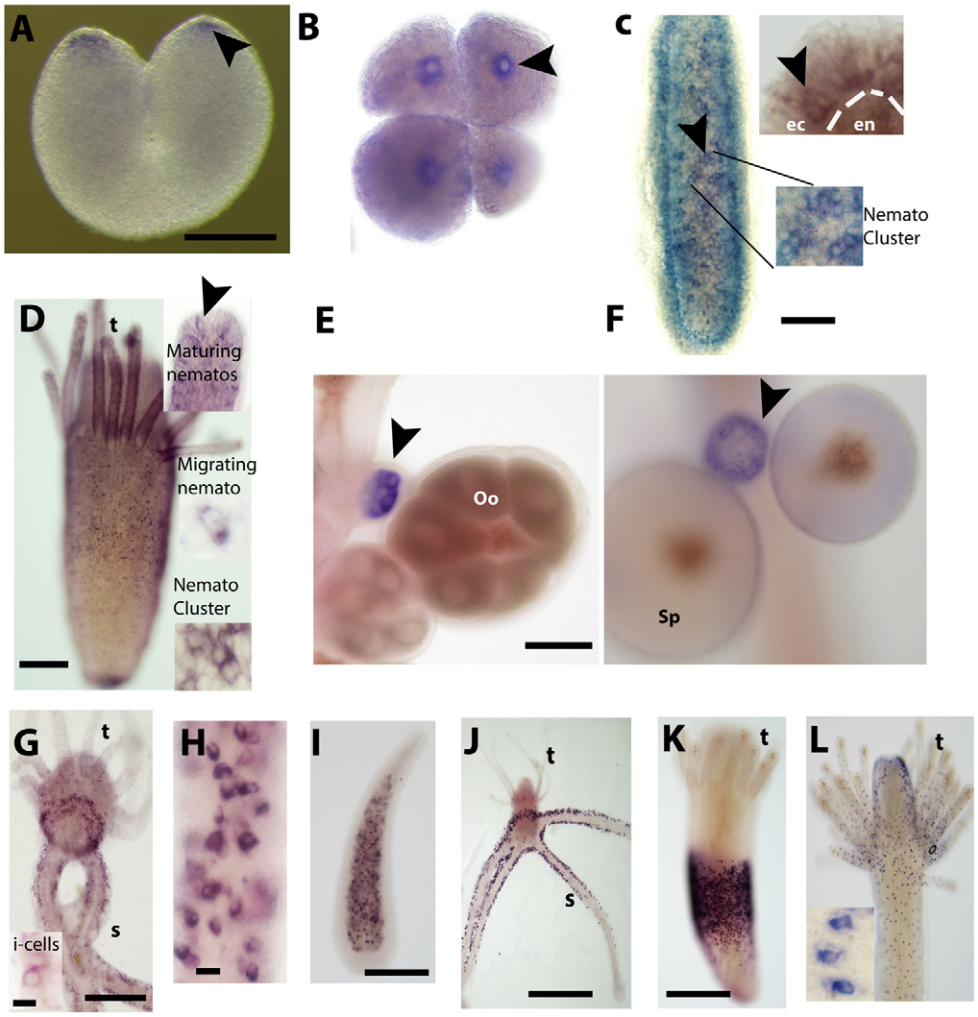

Fig. 2. Expression pattern of *Nanos2*, *Ncol1* and *Rfamide* in normal animals. (**A-G**) *Nanos2* expression. Two-cell (A) and four-cell (B) stage embryos. *Nanos2* is expressed in the prospective oral pole and perinuclear (arrowheads). (C) Preplanula (24 hpf). *Nanos2* is expressed in proliferating nematoblast clusters in the endodermal cell mass (lower inset) and in maturing nematocytes in the ectoderm (higher inset, arrowhead). Dashed line represents the mesoglea. The light blue background results from the surrounding, out of focus, *Nanos2*+ immature nematocytes in the dense interstitial spaces of the ectoderm. (D) Expression in mature feeding polyp. *Nanos2* is expressed in nematoblasts clusters in the lower part (lower inset), in individual migrating nematoblasts (middle inset), and in maturing nematocytes in the tentacles (upper inset). (E,F) Sexual polyps. *Nanos2* is expressed in female (E) and male (F) early germ cells. (G) Expression of *Nanos2* in primary polyp. Inset shows high magnification of putative undifferentiated i-cell. (**H-K**) *Ncol1* expression. (H) Higher magnification of *Ncol1*+ nematoblasts in the endoderm of a 48 hpf embryo. (I) 72 hpf larva. (J) Primary polyp viewed from below. *Ncol1*+ nematoblasts are only visible in the stolons but not in the young polyp's body column. (K) *Ncol1*+ nematoblasts in a mature feeding polyp. (L) *Rfamide*+ neurons in a mature feeding polyp. Inset shows high magnification of three neurons. All animals are oriented with the oral pole up. en, endoderm; ec, ectoderm; Oo, maturing oocyte; Sp, maturing sperm; t, tentacles; s, stolons. Scale bars: 100 µm (A–G,E, F), 50 µm(C), 200 µm (D), 150 µm (G), 10 µm (G inset, H), 180 µm (I), 300 µm.(J), 400 µm. (K).

nematocytes are predominantly found in the 'ectoderm' of the adult, but are of embryonic endodermal origin and migrate to the outer cell layer ('ectoderm' or epidermis) in late embryonic development and metamorphosis. *Nanos2* was also expressed in metamorphosed animals in mitotic nematoblasts clusters at the base of the polyp, in single migrating nematocytes in the upper part of the body column, and in basally positioned, maturing nematocytes in the tentacles (Fig. 2D; supplementary material Fig. S2C). Fully mature nematocytes, recognized by their capsule with coiled tubule and by their apical position, being mounted in battery cells, were devoid of *Nanos2* transcripts; only basally positioned nematocytes were *Nanos2*+ (supplementary material Fig. S2C). In sexual polyps, the *Nanos2* probe marked early developing germ cells in both male and female individuals, but was undetectable in late developing and mature gametes (Fig. 2E,F; supplementary material Fig. S2D). In the stolons, strong *Nanos2* expression was observed in nematoblasts and maturing nematocytes (Fig. 2G), but it was also expressed in cells resembling uncommitted i-cells, based on their very large nucleus and little cytoplasm (Fig. 2G; supplementary material Fig. S2A,B). No *Nanos2* expression was observed in epithelial cells, in contrast to *Nanos2* in *Hydra* (Mochizuki et al., 2000).

Nanos1 was strongly expressed in early developing female gametes (supplementary material Fig. S2E), but never observed in males. Furthermore, its mRNA levels in all other cell types were undetectable by *in situ* hybridization. Noteworthy, in a related cnidarian, *Clytia hemisphaerica*, *CheNanos1* has a similar

expression as *CheNanos2* (Leclère et al., 2012). In *Hydra*, *Nanos1* is expressed in germ cells and in multipotent stem cells (Mochizuki et al., 2000). *Hydractinia Nanos1* has a similar expression pattern as mammalian *Nanos2-3*. However, while mammalian *Nanos2* is male specific, *Hydractinia Nanos1* is female specific. *Hydractinia Nanos2* expression in the nervous system resembles mammalian *Nanos1*. Yet, unlike *Hydractinia Nanos2*, mammalian *Nanos1* is not expressed in germ cells. The *Drosophila* single *nanos* gene is expressed in both germ cells and in the nervous system, similar to *Hydractinia Nanos2*.

Pumilio transcripts were found in germ cells (supplementary material Fig. S2F) and in dividing nematoblasts clusters at the base of polyps (supplementary material Fig. S2G). The cell type in the latter could not be identified definitely, but at least some of the cells had nematoblast morphologies. Hence, *Pumilio* expression overlapped with *Nanos2* in germ cells but only partly in somatic cells.

Because *Nanos2* expression was associated with nematogenesis, we also studied the expression pattern of the known nematocyte lineage marker *Ncol1*, which has not been studied in *Hydractinia* previously. *Ncol1* and other minicollagens are classical cnidarian nematocyte differentiation markers (Kurz et al., 1991). These proteins form part of the nematocyst capsule and are not expressed by any other cell type. Minicollagen mRNA is detectable only in nematogenesis but not in mature nematocytes. *Hydractinia Ncol1* mRNA was first expressed in single, nematoblasts in the endodermal cell mass of 24 hpf embryos and in larvae (Fig. 2H,I), and almost never in clusters of dividing nematoblasts. Young metamorphosed animals had *Ncol1*+ cells primarily in their stolons (Fig. 2J). In mature polyps, *Ncol1* was expressed in a belt-like fashion, primarily in single, post-mitotic nematoblasts and only rarely in proliferating clusters (Fig. 2K). Note, however, that nematogenesis occurs in two different anatomical locations: in the polyps and in the stolons. There is no evidence for migration of mature nematocytes from polyps to the stolons or vice versa, but i-cells, their progenitors, generally migrate from the stolons to developing polyps.

Nematocytes are thought to belong to the cnidarian nervous system (Marlow et al., 2009). We therefore sought a definitive neuronal marker and have chosen the *RFamide precursor* gene (hereafter *Rfamide*). Although not expressed in all *Hydractinia* neurons (Katsukura et al., 2003), *RFamide* is a definitive and most commonly used neuronal marker in cnidarians, and is not expressed in any other cell type (Fig. 2L). A pan-neuronal marker is difficult to identify: *Elav* is also not expressed in all neurons in *Nematostella* (Nakanishi et al., 2012), and with the use of anti-acetylated tubulin antibodies it is difficult to quantify cells by counting because they stain the neurites. The proneural gene *Ash* (known in *Hydra* as *Cnash*) is expressed in both nematoblasts (Grens et al., 1995) and in neurons (Hayakawa et al., 2004).

Given the expression pattern of *Nanos2* in proliferating nematoblasts clusters and in maturing nematocytes, we performed two-color double *in situ* hybridization of *Ncol1* and *Nanos2* to better understand gene expression along nematogenesis (Fig. 3). We found that *Ncol1* and *Nanos2* were largely expressed in distinct domains along the nematocyte differentiation pathway

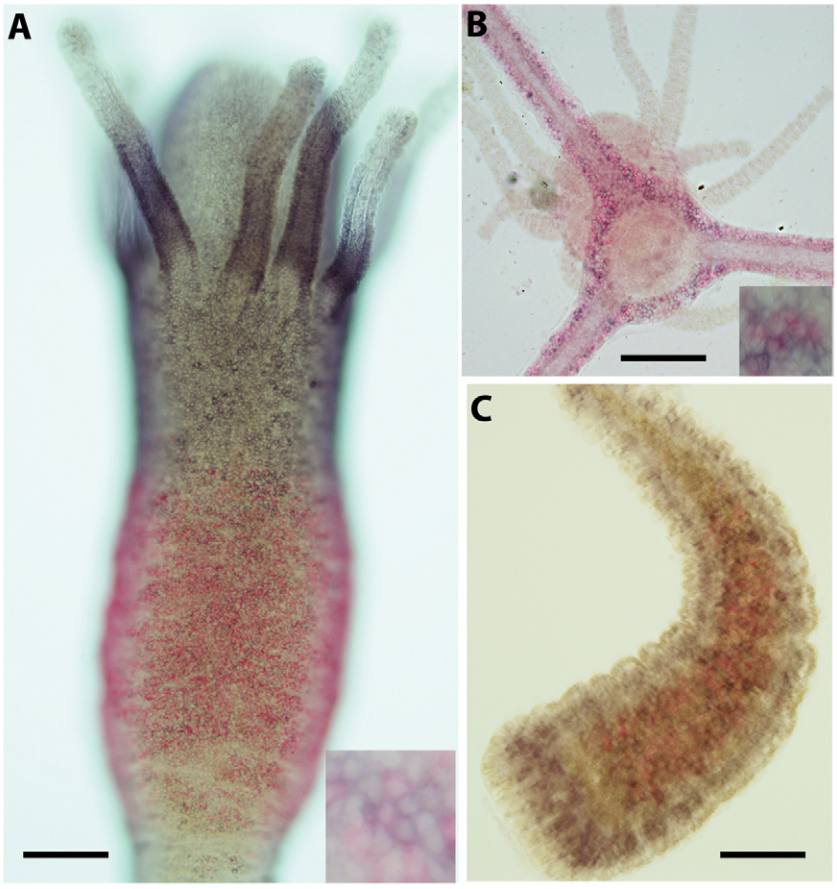

Fig. 3. Double *in situ* hybridization for *Ncol1* and *Nanos2*. (**A**) Overview of a feeding polyp showing only partial overlap in the expression of the two genes; *Ncol1* is stained red and *Nanos2* purple. Inset shows higher magnification of a *Nanos2*-expressing nematoblast cluster where some cells have started to express *Ncol1*. (**B**) Primary polyp growing on a glass slide, viewed from below. Inset shows higher magnification of coexpressing nematoblasts. (**C**) Planula larva showing partially overlapping expression patterns. Scale bars: 200 µm (A,B), 100 µm (C).

with only little overlap at the interface (Fig. 3A). Hence, *Nanos2* is expressed in mitotic nematoblast clusters, but its mRNA dissipates soon after *Ncol1* expression commences. *Nanos2* expression resumes as *Ncol1* transcription ceases and is maintained until late nematocyte maturation, absent from mature nematocytes.

Downregulation of *Nanos2* reduces nematogenesis and increases neurogenesis

The role of Nanos in germ cells is well established in *Drosophila* and in mammals. However, its neuronal role is not well understood. Because *Hydractinia Nanos1* was exclusively expressed in germ cells, whereas *Nanos2* was expressed also in proliferating nematoblasts (which are sensory cells), we decided to study the function of Nanos2. Based on its expression pattern, as described above, we thought that Nanos2 might be required in early nematogenesis. To test this, we used a morpholino antisense oligonucleotide to lower Nanos2 protein levels in embryos. Fertilized eggs were microinjected with a translation block morpholino at 0.25 mM. A scrambled morpholino at the same concentration was used as control (supplementary material Table S1). We found that morphant embryos had a significantly reduced number of *Ncol1* positive nematoblasts (32.5% decrease comparing to control; $P=0.01$; 10 control animals counted and 12 morphants; Fig. 4A) and mature nematocytes in both larvae (37.5% decrease, $P<0.05$; 49 control animals counted and 49 morphants; Fig. 4B) and metamorphosed polyps (50% decrease, $P<0.0001$; 29 control animals and 29 morphants counted; Fig. 4C).

We then analyzed the effect of *Nanos2* downregulation on neurons. This was done by *in situ* hybridization using an *Rfamide* probe. We found that morphants had higher numbers of *Rfamide* positive neurons compared to animals injected with control morpholino (36% increase, $P<0.03$; 7 control larvae counted and 16 morphants; Fig. 4E,F). Note also, that because we work with wild-type, genetically heterogeneous animals the number of neurons varies between individuals. To minimize this effect we performed each experiment on a single batch of sibling animals.

Knocking down of Nanos2 also impacted the morphology of metamorphosed polyps; they had significantly reduced tentacle numbers, from an average of 5.9 tentacles per polyp ($n=32$) in controls, to 1.4 tentacles per polyp ($n=25$) (77% decrease, $P<0.0001$; Fig. 4C,D) in morphants, but appeared normal otherwise.

Hence, downregulation of Nanos2 resulted in decreased number of nematoblasts and nematocytes, but an increase in the number of neurons. It was also associated with a decrease of tentacle numbers post metamorphosis.

The specificity of the morpholino was demonstrated by *in vitro* expression of *Nanos2*-His-tag with the *Nanos2* morpholino and the control morpholino. Western blot using anti-His-tag antibody detected a band at the approximate expected size (37 kDa) in the lane containing the product of the control morpholino but not in the one with the *Nanos2* morpholino (Fig. 4G).

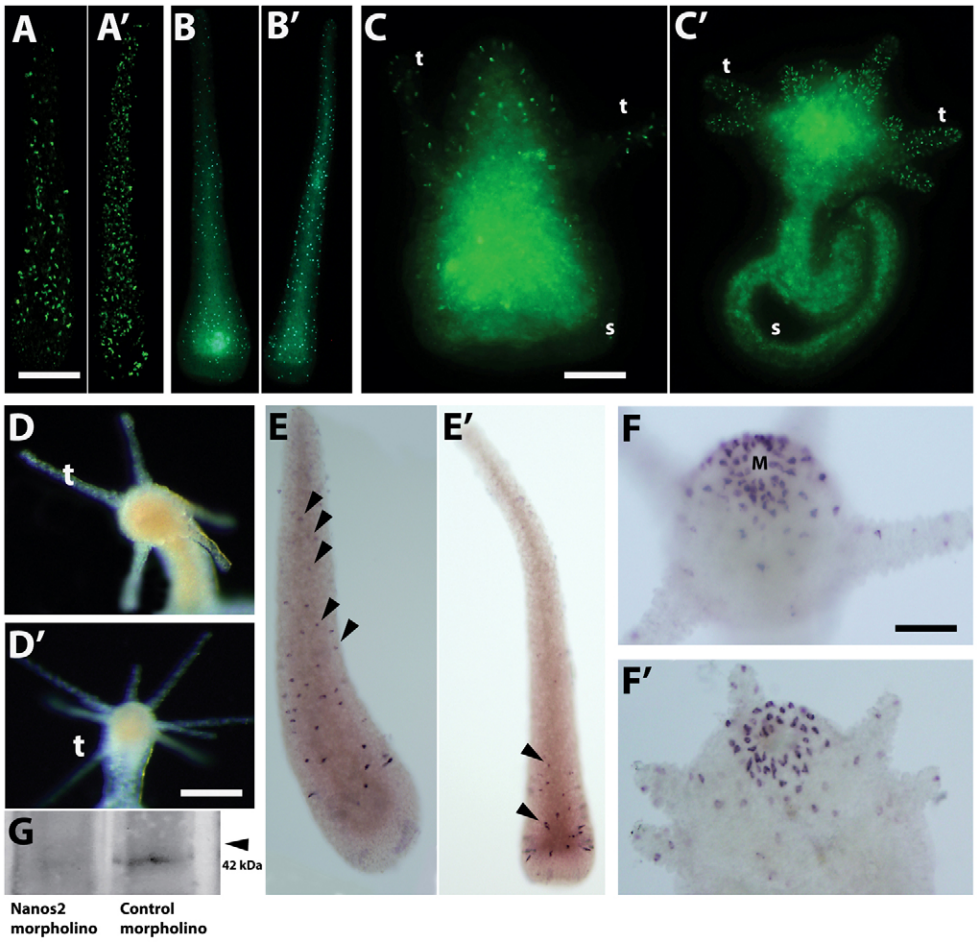

Fig. 4. Morpholino-mediated knockdown of Nanos2. (**A**) NCol1+ nematoblasts in *Nanos2* morphant (A) and control morpholino injected larvae (A′). (**B**) Modified DAPI staining of nematocyst capsules in morphant (B) and control planula larvae (B′). (**C**) Nematocyst capsules in morphant (C) and control metamorphosed primary polyps (C′). (**D**) Tentacle numbers of morphant (D) and control (D′) primary polyps. (**E**) *Rfamide*+ neurons (arrowheads) in morphant (E) and control planulae (E′). (**F**) *Rfamide*+ neurons in morphant (F) and control primary polyps (F′). (**G**) Western blot showing *in vitro* synthesized Nanos2-His-tag in the presence of control morpholino but not with Nanos2 morpholino. t, tentacle; s, stolon. Scale bars: 150 µm.

Ectopic *Nanos2* expression

We then went on to study the effect of excessive *Nanos2* expression. For this, we generated transgenic animals expressing *Nanos2* ectopically. We used a construct consisting of the *Hydractinia Actin1* promoter upstream of the full *Nanos2* coding sequence, fused in-frame with enhanced green fluorescent protein (eGFP) at the 3′ end (supplementary material Fig. S3). The *Hydractinia Actin1* promoter is active ubiquitously in embryogenesis and in the larval stage. However, following metamorphosis its activity switches to become epithelial specific, being quiescent in all other cell types of the animal (Künzel et al., 2010; Millane et al., 2011; Duffy et al., 2012). Hence, using this construct enabled us to study not only the consequences of *Nanos2* ubiquitous overexpression in embryogenesis, but also its long-term effect in epithelial cells that do not express the gene naturally in *Hydractinia*.

Fertilized eggs were microinjected with the construct solution. Stable GFP expression was evident 24–48 hours later (supplementary material Fig. S4A). The integration of the construct into the embryo's genome is a stochastic process and the injected embryos were therefore mosaics (supplementary material Fig. S4A). Animals with a high Nanos2–GFP expression mostly looked distorted, having severe developmental defects, and most of them died before reaching the larval stage (supplementary material Fig. S4B). Those with fewer Nanos2–GFP expressing cells appeared normal. Control animals injected with a construct consisting of the same promoter driving only GFP expression appeared normal independent of the level of their GFP expression (not shown).

Because Nanos2 downregulation compromised nematogenesis, we counted nematoblasts in transgenic embryos, which overexpressed *Nanos2*. Anti-NCol1 antibodies showed, as expected, that the numbers of nematoblasts were significantly higher in *Nanos2* transgenic larvae comparing to wild-type larvae (Fig. 5A; average increase of 110%; $P<0.005$; 33 wild-type

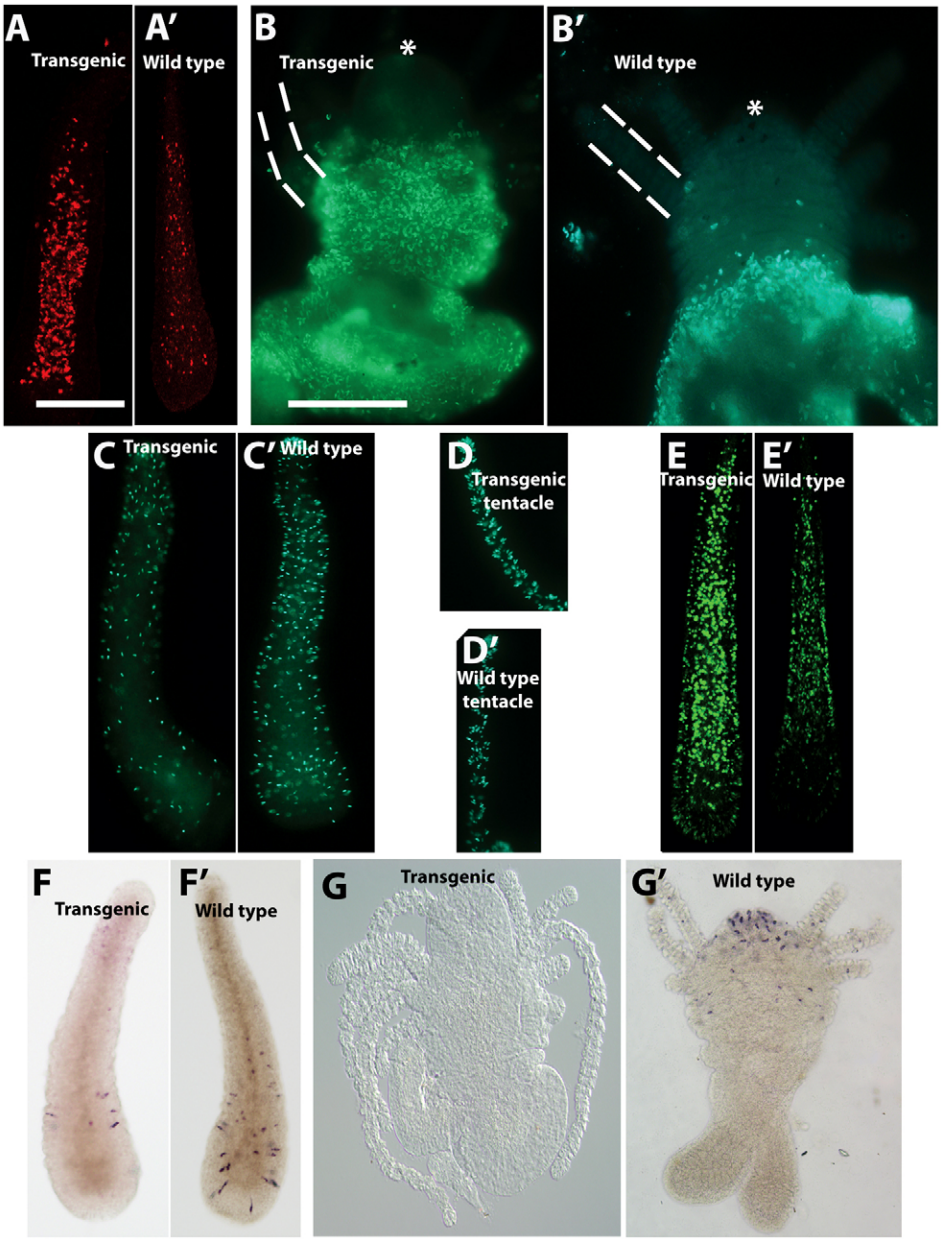

Fig. 5. Gene expression and cellular consequences of *Nanos2* ectopic expression. (**A**,**B**) NCol1 antibody staining of nematoblasts. Transgenic (A) and wild-type (A′) larva. Transgenic (B) and wild-type (B′) primary polyp. Dashed lines indicate the lowest tentacle relative to the mouth (asterisk). (**C**,**D**) Modified DAPI staining to visualize nematocyst capsules in transgenic and wild-type animals. Transgenic (C) and wild-type (C′) larva. Transgenic (D) and wild-type (D′) tentacles of primary polyps. (**E**) BrdU+ cells in transgenic (E) and wild-type (E′) larvae. (**F**,**G**) *Rfamide*+ neurons in transgenic (F) and wild-type larva (F′), and in transgenic (G) and wild-type (G′) metamorphosed primary polyps. Note excessive tentacle number in transgenic polyp. All animals are oriented with their oral poles up. Scale bars: 200 µm.

larvae counted, 34 transgenic ones). Following metamorphosis, when the transgene's expression shifted to epithelial cells and could no longer affect nematogenesis, the numbers of NCol1+ cells was still elevated in 24 hours primary polyps (Fig. 5B; 25% average increase) but was no longer statistically significant ($P=0.1$). The expression domain of NCol1 was also still broadened in transgenic primary polyps as compared to wild-type animals in which NCol1+ nematoblasts were always restricted to the lower part of the polyp body column and never reached the tentacle line. In *Nanos2* transgenic animals, in contrast, we observed NCol1^{+} nematoblasts well above the tentacle line (Fig. 5B). Surprisingly, when we counted the numbers of mature nematocytes in transgenic larvae we discovered that, despite the elevated numbers of nematoblasts, these transgenic embryos and larvae contained significantly fewer mature nematocytes (average decrease of 45%; 11 wild-type and 5 transgenic animals analyzed; $P<0.03$) (Fig. 5C). This trend was reversed in post-metamorphic transgenic animals in which the number of mature nematocytes was higher than in wild-types as expected. Nematocytes were not directly counted in post-metamorphic animals due to their excessive numbers. Instead, we measured their average density and found no significant differences between transgenic and wild-type polyps (Fig. 5D). As transgenic polyps had more tentacles (see below), we concluded that nematocyte numbers were proportionately higher in transgenic animals.

To study the source of the excessive nematoblast numbers in *Nanos2* transgenic larvae, we compared the numbers of S-phase cells in transgenic versus wild-type embryos by BrdU labeling. We found that transgenic animals overexpressing *Nanos2* had significantly higher numbers of BrdU positive cells than wild-type animals (Fig. 5E; 90.5% increase; $P<0.0001$; 19 wild-type embryos counted; 18 transgenic ones).

We then looked at the numbers of neurons. We found that the numbers of *Rfamide* positive neurons were significantly reduced in transgenic embryos, larvae and metamorphosed polyps (average of 83% decrease in larvae, 22 wild-types counted, 25 transgenic animals; $P<0.0001$; Fig. 5F,G).

In addition to the changes in nematoblasts and neurons numbers, metamorphosed animals also displayed abnormal morphologies. The mildest phenotypes was supernumerary, but correctly positioned, tentacles (Fig. 6A,B). Their numbers increased significantly from an average of 9.32 tentacles per wild-type polyp ($n=54$) to 14.28 in transgenic ones ($n=34$)

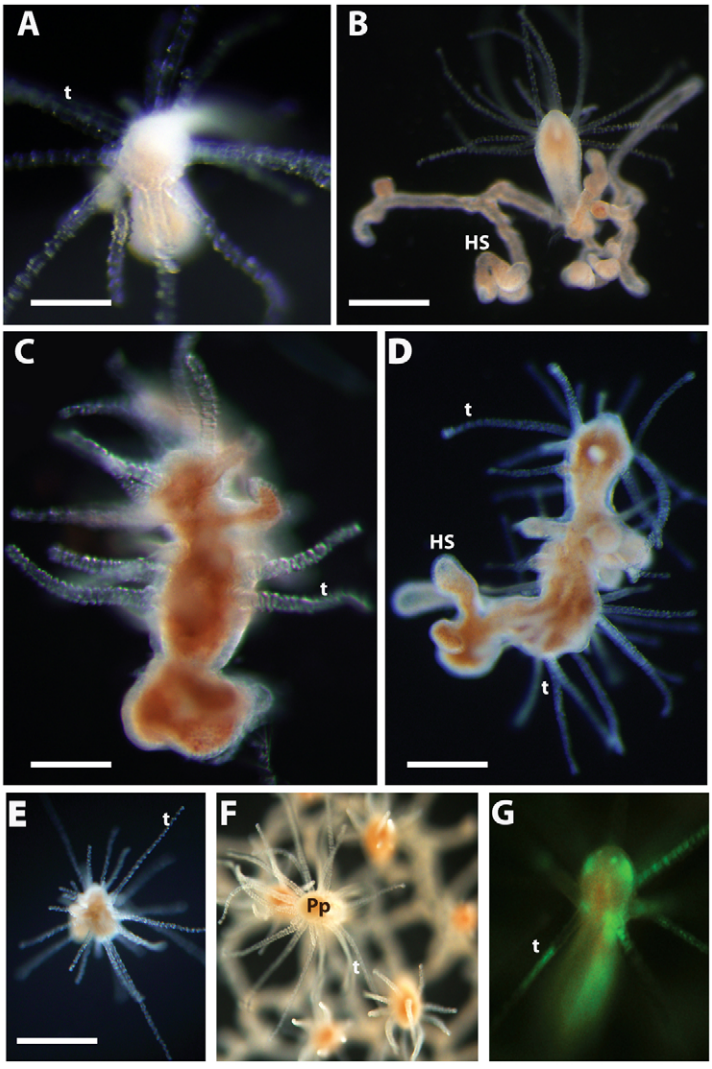

Fig. 6. Consequences of *Nanos2* overexpression. (**A**,**B**) Young metamorphosed polyps with supernumerary tentacles positioned normally around the mouth. (B) Hyperplastic stolons in metamorphosed polyp. (**C**,**D**) Supernumerary and ectopic tentacles in young metamorphosed polyps. (**E**) Primary polyp comprising a ball with tentacles and no other structure. (**F**) Transgenic colony several weeks post metamorphosis. The primary polyp still displays supernumerary tentacles, but all secondary, genetically identical polyps have normal tentacle numbers. Stolons are shown out of focus. (**G**) Transgenic secondary polyp expressing Nanos2-GFP in its epithelial cells but display normal morphology. All animals are oriented with the oral pole up except in F, which was photographed from above. t, tentacles; HS, hyperplastic stolon, Pp, primary polyp. Scale bars: 200 µm (A), 300 µm (B), 180 µm (C), 250 µm (D), 350 µm (E).

(increase of 53% in transgenic animals; $P<0.0001$). This abnormal phenotype was not evident immediately post metamorphosis, but required at least one week to develop. A more severe phenotype was observed in polyps which had not only supernumerary tentacles but also grew them ectopically down the body column (Fig. 6C,D). All ectopic tentacles had normal morphologies, contained numerous stinging cells (nematocytes) mounted in epithelial battery cells, and were fully functional as attested by their ability to kill brine shrimp nauplii. Many transgenic animals also developed hyperplastic stolons (Fig. 6B,D). In normal animals, these organs form as temporarily modified stolons during allogeneic encounters between histoincompatible animals (Ivker, 1972; McFadden et al., 1984; Lange et al., 1989; Lange, et al., 1992; Müller, 2002). Hyperplastic stolons are swollen by excessive nematocytes that are used to inflict damage on allogeneic tissues. However, transgenic animals were not exposed to a direct contact with other colonies. Finally, three animals developed as a ball of tentacles without any further structure (Fig. 6E).

Following metamorphosis, the transgene's expression became restricted to epithelial tissue, and expression in other transgenic cells had shut down. Concomitantly, the phenotypes of the animals gradually dissipated over the next weeks and all newly budded clonal polyps after the primary polyp (*i.e.* the first polyp that emerges during metamorphosis) appeared completely normal despite strong Nanos2–GFP expression in their epithelia (Fig. 6F,G). Nevertheless, up to several weeks later, the first polyp in these colonies was still recognizable due to its excessive tentacle number (Fig. 6F), comparing to its genetically identical clone mates that had normal tentacle numbers.

Nanos2 mediated excessive tentacle development is Wnt independent

In cnidarians, anterior–posterior polarity is controlled by canonical Wnt signaling. Ectopic activation of the canonical Wnt pathway induces ectopic tentacles (Lee et al., 2006; Plickert et al., 2006; Duffy et al., 2010), reminiscent of the *Nanos2* mediated excessive tentacles shown here. To investigate a possible involvement of Nanos2 in Wnt mediated axial patterning we studied the expression of *Wnt3* in transgenic animals. This gene is expressed exclusively in the oral pole of *Hydractinia* throughout its life cycle and is a known target of its own protein through canonical Wnt signaling. Consequently, global activation of canonical Wnt signaling deregulates *Wnt3*, rendering it ubiquitous (Plickert et al., 2006; Duffy et al., 2010). We thought that if Nanos2 were upstream of Wnt, then *Nanos2* transgenic animals should also have a depolarized, more ubiquitous *Wnt3* expression. However, the expression of *Wnt3* in transgenic animals remained restricted to the very oral end as in wild-type polyps and no *Wnt3* mRNA was detected anywhere else in the animal (Fig. 7A,B). This shows that Nanos2 does not affect canonical Wnt signaling, and that the ectopic tentacle formation in *Nanos2* transgenic animals was likely Wnt independent.

Conversely, ectopic Wnt activation by treatment with azakenpaullone, a specific inhibitor of Gsk3 (Kunick et al., 2004; Müller et al., 2004b; Teo et al., 2006), drove ubiquitous *Nanos2* expression (Fig. 7C,D), suggesting that *Nanos2* is a putative downstream target of canonical Wnt signaling.

Discussion

Nanos is a classical germ cell marker in virtually all animals (Ewen-Campen et al.). Its general mode of action is the inhibition

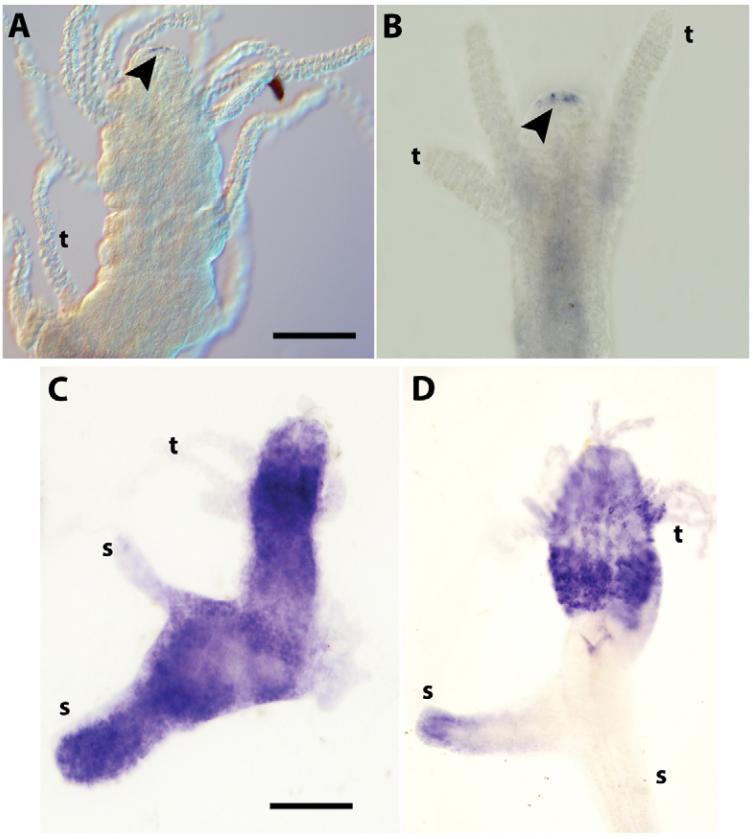

Fig. 7. Relation between *Nanos2* and canonical Wnt signaling. (**A**) *Nanos2* transgenic primary polyp expressing *Wnt3* only at the very oral tip (arrowhead). (**B**) Normal polyp with similar *Wnt3* expression pattern. (**C**) Ubiquitous *Nanos2* expression in primary polyp treated with azakenpaullone to ectopically activate canonical Wnt signaling. (**D**) *Nanos2* expression in control, untreated animal. t, tentacle; s, stolon. Scale bars: 150 µm (A), 200 µm (C).

of translation of its target mRNAs, but it can also mediate mRNA degradation by recruiting deadenylating enzymes (Kadyrova et al., 2007). The role of Nanos in germ cells is well documented, based on work done on flies and mice. Because both *Hydractinia Nanos* homologs were expressed in germ cells it is reasonable to assume that they function similarly in this context.

Less understood is the role of Nanos in the nervous system. In *Drosophila*, Nanos has been associated with dendrite morphogenesis (Ye et al., 2004; Brechbiel and Gavis, 2008), with presynaptic terminal growth, and with postsynaptic glutamate receptor subunit composition (Kadyrova et al., 2007). In the mouse, only one out of three Nanos homologues (Nanos1) is expressed in the nervous system. The function of which, however, is unknown, as its complete absence causes no visible developmental abnormality. By contrast, Nanos' canonical partner, Pumilio, does function in the mammalian nervous system (Vessey et al., 2010; Marrero et al., 2011; Siemen et al., 2011). Because Nanos and Pumilio usually act in concert, the role of Nanos in the mammalian nervous system might have been overlooked, owing perhaps to the complexity of the mammalian nervous system. The by far simpler nervous system of *Hydractinia* may be more informative in studying Nanos functions.

Indeed, our results point to a novel and unexpected role for Nanos in neural cell fate determination. *Nanos2* overexpression resulted in increased numbers of nematoblasts, by increasing their proliferation, but decreased numbers of mature nematocytes in pre and early post metamorphosis stages. This suggests that Nanos2 also acts in inhibiting nematocyte maturation. An additional role of Nanos2 in late nematocyte differentiation may be related to migration. Hence, while promoting nematoblast migration, Nanos2 may prevent their last maturation stages until the cells reach their final destination in the tentacles where they lose *Nanos2* expression, stop migrating and fully mature. This is consistent with its expression pattern in these cells (Fig. 2C,D; supplementary material Fig. S2A–D), and explains why *Hydractinia* larvae overexpressing *Nanos2* had only few mature nematocytes despite having an excess of *Ncol1*+ progenitors, until after metamorphosis when the transgene's expression became solely epithelial. Transgenic animals had, in contrast, lower numbers of *Rfamide*+ neurons in both pre- and post-metamorphic stages. Although we have no definite marker for early neuroblasts, it is unlikely that neuroblasts numbers were increased and merely their maturation inhibited by ectopic Nanos2, as in the case of nematoblasts. If this were the case, increased numbers of *Rfamide*+ neurons should have been produced post metamorphosis, similar to nematocytes, which was not the case. Therefore, *Nanos2* expression was key in determining the balance between nematocytes and *Rfamide*+ neurons. Nanos2 may be acting on i-cells, promoting them to become committed to nematogenesis and also promotes their proliferation following commitment. This would result in a decrease in other i-cell derivatives, such as neurons. We have not counted other cell types but cannot exclude that numbers of other cell types would be affected too. Alternatively, *Nanos2* could act on a common nematocyte neural progenitor, affecting only nematocytes and neurons. The existence of such a cell has been proposed previously (Miljkovic-Licina et al., 2007). The results of *Nanos2* expression manipulation are summarized in Fig. 8A.

Although Nanos seems to be involved in posterior patterning in many insects (Lall et al., 2003), evidence for a similar function in other animals is scarce, and based exclusively on polarized Nanos expression patterns in various animals such as leeches (Pilon and Weisblat, 1997), *Hydractinia* (this study) and other cnidarians (Mochizuki et al., 2000; Torras et al., 2004; Extavour et al., 2005; Torras and González-Crespo, 2005; Leclère et al., 2012). The presence of the ectopic tentacles of post metamorphic *Nanos2* transgenic animals could support a similar role in cnidarians, as tentacles are oral structures and the cnidarian head corresponds to the larval posterior pole (Meinhardt, 2002). However, six lines of evidence dispute this hypothesis: First, although *Nanos* transcripts were concentrated at the prospective oral pole of the early embryo (Fig. 2A), in gastrulae and larval stages *Nanos2* expression was not polarized (Fig. 2C). Second, the only evidence for polarity defects (*i.e.* ectopic tentacles) became evident post-metamorphosis, concomitant with the increasing numbers of mature nematocytes (Figs 5,6). In contrast, ectopic Wnt activation in *Hydractinia* embryos oralizes the animals already at the pre-larva stage (Plickert et al., 2006), different from ectopic *Nanos2* expression. Third, with the exception of three cases (out of 25), *Nanos2* ectopic expression did not cause polarity defects other than extra tentacles (Fig. 6). Fourth, *Nanos2* downregulation had no effect on axis polarity except of lowering nematocyte and tentacle numbers (Fig. 4). Fifth, long-term surviving transgenic animals had normal morphologies despite ectopic Nanos2 in their epithelial cells (Fig. 6F,G). Finally, expression of *Wnt3*, a major regulator of cnidarian axis polarity, was unaltered in *Nanos2* transgenic animals (Fig. 7A,B), showing that Nanos2 mediated ectopic tentacles are Wnt-independent. Hence, we favor the hypothesis that excessive numbers of nematocytes, rather than polarity defects, drove extra tentacle formation, but cannot exclude the alternative hypothesis. Of note, i-cell (and therefore nematocyte) free *Hydra* can regenerate tentacles (Marcum and Campbell, 1978; Sugiyama and Fujisawa, 1978), but recent studies showed that neurogenesis is requited for head (hence, tentacle) regeneration of normal *Hydra* (Miljkovic-Licina et al., 2007). In *Hydractinia*, elimination of i-cells results in tentacles, and eventually polyps, being resorbed (Müller et al., 2004a). Hence, nematocytes may have a role in normal cnidarian tentacle formation.

A model summarizing Nanos2 function in nematogenesis is presented in Fig. 8B. Analysis of *Nanos2* expression pattern and functional studies suggest that *Nanos2* is expressed in two distinct phases of nematogenesis. In the first, it promotes i-cells commitment to nematocytes and represses neuronal fate. During this phase, Nanos2 is likely to act in concert with its partner, Pumilio, as their expression patterns overlap in early nematoblasts. Later, as nematoblasts exit the cell cycle, *Nanos2* transcription is silenced and replaced by *Ncol1*. At the end of the *Ncol1* phase, *Nanos2* expression resumes until stinging cells mature. In later nematocyte development Nanos2 promotes migration of maturing nematocytes, but prevents their final maturation until they reach their final destination. *Nanos2* and *Pumilio* expression patterns, overlapping only in proliferating nematoblasts, may suggest that Nanos acts independent of Pumilio in the later phase of nematocytes development.

Taken together, Nanos was shown previously to have a conserved role in germ stem cell maintenance, self-renewal, migration, and prevention of differentiation. Our data add a similar role for Nanos in a neural lineage, and suggest it has no direct role in cnidarian axis patterning, a role that might be an insect or arthropod innovation.

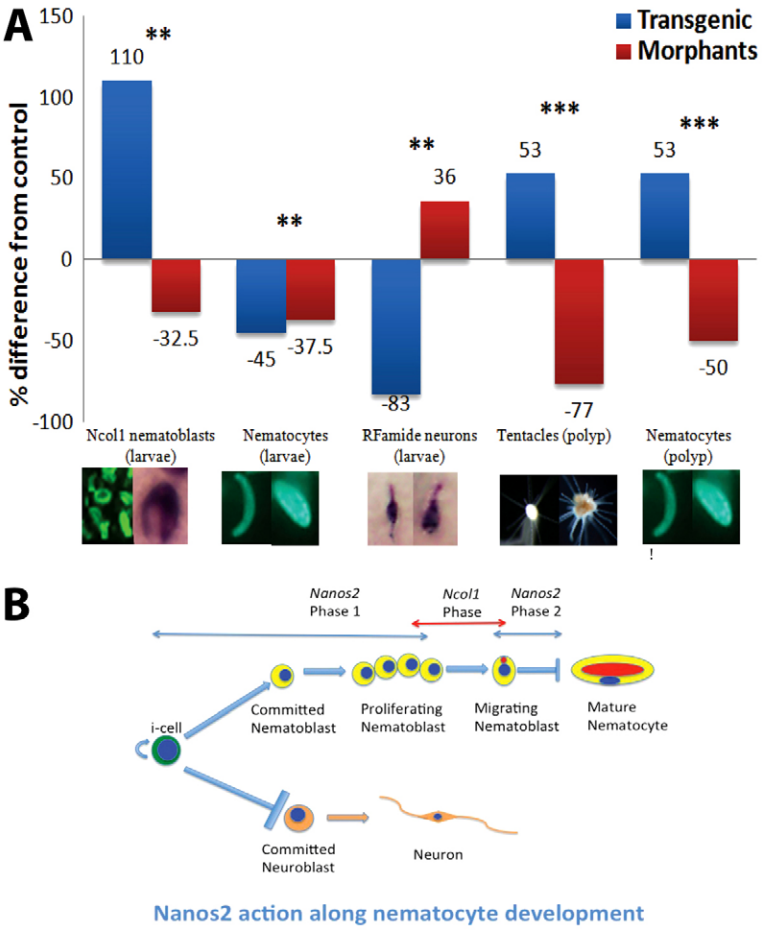

Fig. 8. Summary of the effects of *Nanos2* misexpression and its role in *Hydractinia*. (**A**) Summary of effects; $^{**}P<0.05$, $^{***}P<0.0001$. (**B**) Model for the role of Nanos2 in nematogenesis. *Nanos2* is expressed in two distinct phases of nematogenesis. In the first phase, it acts on i-cells, promoting nematocytes and repressing neuronal fate. It then promotes proliferation of committed nematoblasts. As nematoblasts exit the cell cycle, *Nanos2* transcription stops and is replaced by *Ncol1*. At the end of the *Ncol1* phase, *Nanos2* expression resumes. Nanos2 then acts to promote migration of maturing nematocytes, but prevents their final maturation until they reach their final destination, mounted in battery cells, where *Nanos2* mRNA dissipates and the cells fully mature. Blue circles or ellipsoids represent nuclei. Red circle represents developing nematocyst capsule and the red ellipsoid represents mature nematocyst capsule.

Materials and Methods

Animal culture

Animals were collected in Galway Bay by SCUBA, and cultured in seawater. They were fed brine shrimp nauplii five times a week supplemented by ground fish once a week. Embryos were collected about an hour following light-induced spawning. Metamorphosis was induced by a pulse treatment in 100 mM CsCl (Müller and Buchal, 1973).

In situ hybridization

In situ hybridization was performed as described (Gajewski et al., 1996). DIG- and Fluorescein labeled RNA probes (Roche) were synthesized using SP6 and T7 RNA polymerases according to the manufacturer's protocol (Fermentas). *In situ* hybridization was performed at 50°C. For fluorescent *in situ* hybridization we followed the protocol by Toledano et al. (Toledano et al., 2012).

Generation of transgenic animals

We prepared a vector consisting of the *Hydractinia Actin1* promoter, driving expression of *Nanos2* fused in frame with enhanced green fluorescent protein (supplementary material Fig. S3). One-two cell stage embryos were microinjected with 200 pl volume of the plasmid at a concentration of 4–5 µg/µl as previously described (Künzel et al., 2010; Duffy et al., 2012; Millane et al., 2011).

Morpholino-mediated downregulation

Fluorescein conjugated translation block morpholino oligonucleotides (see supplementary material Table S1 for sequence) were designed and synthesized by Gene Tools. One-two cell stage embryos were microinjected with 100 pl at 0.25–0.5 mM. As a control scrambled morpholinos were injected at the same concentration.

Western Blotting was performed to verify the specificity of the translation block morpholino oligonucleotide. For this purpose, Nanos2-His-tag protein was synthesized using the *in vitro* transcription-translation system TNT®T7 Coupled Reticulocyte Lysate System (Promega, cat.no. L4611). We added 1 µl of 1 mM *Nanos2* morpholino to 50 µl transcription-translation reaction. As control, a transcription-translation reaction was performed with the non-coding scrambled morpholino. Synthesized, His-tagged proteins were detected using rabbit anti-His-tag antibodies (1:1000 dilution, Santa Cruz, cat no. SC-803), followed by HRP-conjugated Goat anti-rabbit IgG (1:1000 dilution, Invitrogen, cat. no. 656120) and a chemiluminescent substrate.

Immunohistochemistry

Animals were fixed in 4% paraformaldehyde in PBS for 60 minutes and then dehydrated in ethanol through four steps (25, 50, 75 and 100%). Samples were rehydrated and blocked for 30 minutes in 2% BSA in PBS (BSA/PBS), then blocked for 30 minutes in 5% goat serum in BSA/PBS (GS/BSA/PBS). The antibody was diluted 1:500 in GS/BSA/PBS and incubated for 1 hour at room temperature, followed by three washes with BSA/PBS and re-blocking as above. Pre-adsorbed secondary antibodies (Alexa Fluor 594 and 488 goat anti-rabbit IgG, cat. no. A-11012 and A-11008, Invitrogen) were diluted 1:500 in GS/BSA/PBS and incubated for 1 hour at room temperature. Animals were mounted in 90% glycerol/PBS.

BrdU staining

Animals were incubated in seawater containing 200 mM BrdU for 1 hour and then washed with seawater. Forty minutes later they were fixed with paraformaldehyde. The specimens were washed in PBS, then with 0.4 M glycine pH7.2. Next they were treated with 2 M HCl, then washed with 0.25% Triton PBS. Unspecific binding of the antibodies was blocked with 1% BSA in 0.25% Triton PBS. Samples were then incubated for 1 hour at room temperature in 1:500 dilution of anti-BrdU (Roche), then washed with 0.25% Triton PBS and incubated in the dark at room temperature for 1 hour in pre-absorbed 1:500 dilution of secondary antibody, Alexa Fluor 488 anti-mouse antibody (Invitrogen, cat. no. A11059). Finally, they were washed with 0.25% Triton PBS and mounted in glycerol.

Labeling and counting of cells

Nematoblasts

Stinging cell progenitors were visualized using the rabbit polyclonal anti *Hydra* NCol1 antibody (Adamczyk et al., 2010), a kind gift from Dr Suat Özbek (University of Heidelberg, Germany). The numbers of nematoblasts were too high to be counted in full. We therefore counted all NCol1+ cells in a single, anterior-posterior confocal

plane, choosing the one with the highest number of cells in each counted animal. Statistical analyses were performed by the two-sample Student's *t*-test method using the Minitab software.

Nematocysts

Mature nematocytes were counted by staining the poly-γ-glutamate contents of their nematocyst capsules with DAPI as described (Szczepanek et al., 2002) and viewing them under the FITC channel of a confocal microscope. Under these conditions only nematocyst capsules, and not nuclei, were visible. Nematocysts in embryos and larvae were counted in full confocal z-stacks of the entire animals. Counting nematocysts in animals older than a week post metamorphosis is difficult due to their high numbers and distribution among the different animal compartments (tentacles, body column and stolons). As alternative, we counted nematocysts in the most distal 80 µm of 24 wild-type and 9 *Nanos2* transgenic tentacles but found no significant difference between them (9% increase in transgenic animals $P=0.119$). We therefore took the number of tentacles in a polyp as a proxy for the total number of nematocysts.

S-phase cells

All BrdU+ cells per animal were counted for single confocal layer, choosing the one with the highest number of cells in each counted animal.

Rfamide+ neurons

Neurons expressing *Rfamide* were visualized by *in situ* hybridization. We counted all the cells in the animals using brightfield microscopy.

Phylogenetic analyses

Nanos protein sequences from various animals were taken from GenBank and boundaries of their conserved domains were established based on a previously described phylogenetic analysis (Extavour et al., 2005). Alignment of conserved domains was prepared using ClustalW2 (http://www.ebi.ac.uk/Tools/msa/clustalw2) and adjusted manually. Bootstrapped (100 replicates) phylogenetic tree of Nanos was inferred by the MEGA 5.10 software, using the maximum likelihood method with the Jones-Taylor-Thornton (JTT) model of amino acid substitution and the Nearest-Neighbor-Interchange (NNI) method, and prepared using the NJ/BioNJ option.

Acknowledgements

We thank members of the Frank laboratory for their continuous support and discussions. Albert Lawless, Eoin MacLoughlin, John Galvin and Terry Callanan are kindly acknowledged for technical assistance. Anti-NCol1 antibody was a kind gift from Suat Özbek (University of Heidelberg).

Author contributions

J.K. and U.F. designed the experiments, J.K. performed the experiments, and J.K. and U.F. wrote the paper.

Funding

U.F. is a Science Foundation Ireland (SFI) Principal Investigator [grant numbers 07/IN.1/B943 and 11/PI/1020]. J.K. was a recipient of a Thomas Crawford Hayes Fund award in support of her PhD dissertation.

Supplementary material available online at
http://jcs.biologists.org/lookup/suppl/doi:10.1242/jcs.127233/-/DC1

References

Adamczyk, P., Zenkert, C., Balasubramanian, P. G., Yamada, S., Murakoshi, S., Sugahara, K., Hwang, J. S., Gojobori, T., Holstein, T. W. and Özbek, S. (2010). A non-sulfated chondroitin stabilizes membrane tubulation in cnidarian organelles. *J. Biol. Chem.* **285**, 25613-25623.

Brechbiel, J. L. and Gavis, E. R. (2008). Spatial regulation of nanos is required for its function in dendrite morphogenesis. *Curr. Biol.* **18**, 745-750.

Chapman, J. A., Kirkness, E. F., Simakov, O., Hampson, S. E., Mitros, T., Weinmaier, T., Rattei, T., Balasubramanian, P. G., Borman, J., Busam, D. et al. (2010). The dynamic genome of *Hydra*. *Nature* **464**, 592-596.

Duffy, D. J., Plickert, G., Kuenzel, T., Tilmann, W. and Frank, U. (2010). Wnt signaling promotes oral but suppresses aboral structures in *Hydractinia* metamorphosis and regeneration. *Development* **137**, 3057-3066.

Duffy, D. J., Millane, R. C. and Frank, U. (2012). A heat shock protein and Wnt signaling crosstalk during axial patterning and stem cell proliferation. *Dev. Biol.* **362**, 271-281.

Ewen-Campen, B., Schwager, E. E. and Extavour, C. G. (2010). The molecular machinery of germ line specification. *Mol. Reprod. Dev.* **77**, 3-18.

Extavour, C. G., Pang, K., Matus, D. Q. and Martindale, M. Q. (2005). vasa and nanos expression patterns in a sea anemone and the evolution of bilaterian germ cell specification mechanisms. *Evol. Dev.* **7**, 201-215.

Freeman, G. (1981). The role of polarity in the development of the hydrozoan planula larva. *Rouxs Arch. Dev. Biol.* **190**, 168-184.

Gajewski, M., Leitz, T., Schlossherr, J. and Plickert, G. (1996). LWamides from Cnidaria constitute a novel family of neuropeptide with morphogenetic ativity. *Rouxs Arch. Dev. Biol.* **205**, 232-242.

Galliot, B., Quiquand, M., Ghila, L., de Rosa, R., Miljkovic-Licina, M. and Chera, S. (2009). Origins of neurogenesis, a cnidarian view. *Dev. Biol.* **332**, 2-24.

Grens, A., Mason, E., Marsh, J. L. and Bode, H. R. (1995). Evolutionary conservation of a cell fate specification gene: the *Hydra* achaete-scute homolog has proneural activity in *Drosophila*. *Development* **121**, 4027-4035.

Haraguchi, S., Tsuda, M., Kitajima, S., Sasaoka, Y., Nomura-Kitabayashid, A., Kurokawa, K. and Saga, Y. (2003). nanos1: a mouse nanos gene expressed in the central nervous system is dispensable for normal development. *Mech. Dev.* **120**, 721-731.

Hayakawa, E., Fujisawa, C. and Fujisawa, T. (2004). Involvement of *Hydra* achaete-scute gene CnASH in the differentiation pathway of sensory neurons in the tentacles. *Dev. Genes Evol.* **214**, 486-492.

Hayashi, Y., Hayashi, M. and Kobayashi, S. (2004). Nanos suppresses somatic cell fate in Drosophila germ line. *Proc. Natl. Acad. Sci. USA* **101**, 10338-10342.

Ivker, F. B. (1972). A hierarchy of histo-incompatibility in *Hydractinia echinata*. *Biol. Bull.* **143**, 162-174.

Juliano, C. E., Swartz, S. Z. and Wessel, G. M. (2010). A conserved germline multipotency program. *Development* **137**, 4113-4126.

Kadyrova, L. Y., Habara, Y., Lee, T. H. and Wharton, R. P. (2007). Translational control of maternal Cyclin B mRNA by Nanos in the Drosophila germline. *Development* **134**, 1519-1527.

Katsukura, Y., David, C. N., Grimmelikhuijzen, C. J. and Sugiyama, T. (2003). Inhibition of metamorphosis by RFamide neuropeptides in planula larvae of *Hydractinia echinata*. *Dev. Genes Evol.* **213**, 579-586.

Kunick, C., Lauenroth, K., Leost, M., Meijer, L. and Lemcke, T. (2004). 1-Azakenpaullone is a selective inhibitor of glycogen synthase kinase-3 beta. *Bioorg. Med. Chem. Lett.* **14**, 413-416.

Künzel, T., Heiermann, R., Frank, U., Müller, W. A., Tilmann, W., Bause, M., Nonn, A., Helling, M., Schwarz, R. S. and Plickert, G. (2010). Migration and differentiation potential of stem cells in the cnidarian *Hydractinia* analysed in eGFP-transgenic animals and chimeras. *Dev. Biol.* **348**, 120-129.

Kurz, E. M., Holstein, T. W., Petri, B. M., Engel, J. and David, C. N. (1991). Mini-collagens in *hydra* nematocytes. *J. Cell Biol.* **115**, 1159-1169.

Lall, S., Ludwig, M. Z. and Patel, N. H. (2003). Nanos plays a conserved role in axial patterning outside of the Diptera. *Curr. Biol.* **13**, 224-229.

Lange, R., Plickert, G. and Mueller, W. A. (1989). Histoincompatibility in a low invertebrate, *Hydractinia echinata*: Analysis of the mechanisms of rejection. *J. Exp. Zool.* **249**, 284-292.

Lange, R. G., Dick, M. H. and Müller, W. A. (1992). Specificity and early ontogeny of historecognition in the hydroid *Hydractinia*. *J. Exp. Zool.* **262**, 307-316.

Leclère, L., Jager, M., Barreau, C., Chang, P., Le Guyader, H., Manuel, M. and Houliston, E. (2012). Maternally localized germ plasm mRNAs and germ cell/stem cell formation in the cnidarian Clytia. *Dev. Biol.* **364**, 236-248.

Lee, P. N., Pang, K., Matus, D. Q. and Martindale, M. Q. (2006). A WNT of things to come: evolution of Wnt signaling and polarity in cnidarians. *Semin. Cell Dev. Biol.* **17**, 157-167.

Lehmann, R. and Nüsslein-Volhard, C. (1991). The maternal gene nanos has a central role in posterior pattern formation of the *Drosophila* embryo. *Development* **112**, 679-691.

Lindgens, D., Holstein, T. W. and Technau, U. (2004). Hyzic, the *Hydra* homolog of the zic/odd-paired gene, is involved in the early specification of the sensory nematocytes. *Development* **131**, 191-201.

Marcum, B. A. and Campbell, R. D. (1978). Development of *Hydra* lacking nerve and interstitial cells. *J. Cell Sci.* **29**, 17-33.

Marlow, H. Q., Srivastava, M., Matus, D. Q., Rokhsar, D. S. and Martindale, M. Q. (2009). Anatomy and development of the nervous system of Nematostella vectensis, an anthozoan cnidarian. *Dev. Neurobiol.* **69**, 235-254.

Marrero, E., Rossi, S. G., Darr, A., Tsoulfas, P. and Rotundo, R. L. (2011). Translational regulation of acetylcholinesterase by the RNA-binding protein Pumilio-2 at the neuromuscular synapse. *J. Biol. Chem.* **286**, 36492-36499.

McFadden, C. S., McFarland, M. J. and Buss, L. W. (1984). Biology of hydractiniid hydroids. I. Colony ontogeny in *Hydractinia echinata* (Fleming). *Biol. Bull.* **166**, 54-67.

Meinhardt, H. (2002). The radial-symmetric *hydra* and the evolution of the bilateral body plan: an old body became a young brain. *Bioessays* **24**, 185-191.

Miljkovic-Licina, M., Chera, S., Ghila, L. and Galliot, B. (2007). Head regeneration in wild-type *hydra* requires de novo neurogenesis. *Development* **134**, 1191-1201.

Millane, R. C., Kanska, J., Duffy, D. J., Seoighe, C., Cunningham, S., Plickert, G. and Frank, U. (2011). Induced stem cell neoplasia in a cnidarian by ectopic expression of a POU domain transcription factor. *Development* **138**, 2429-2439.

Mochizuki, K., Sano, H., Kobayashi, S., Nishimiya-Fujisawa, C. and Fujisawa, T. (2000). Expression and evolutionary conservation of nanos-related genes in *Hydra*. *Dev. Genes Evol.* **210**, 591-602.

Müller, W. A. (2002). Autoaggressive, multi-headed and other mutant phenotypes in *Hydractinia echinata* (Cnidaria: Hydrozoa). *Int. J. Dev. Biol.* **46**, 1023-1033.
Müller, W. A. and Buchal, G. (1973). Metamorphoseinduktion bei planulalarven. II. Induktion durch monovalente kationen: die bedeutung des Gibbs-Donnan verhältnisses und der Ka+Na+-ATPase. *Wilhelm Roux's Arch.* **173**, 122-135.
Müller, W. A., Teo, R. and Frank, U. (2004a). Totipotent migratory stem cells in a hydroid. *Dev. Biol.* **275**, 215-224.
Müller, W. A., Teo, R. and Möhrlen, F. (2004b). Patterning a multi-headed mutant in *Hydractinia*: enhancement of head formation and its phenotypic normalization. *Int. J. Dev. Biol.* **48**, 9-15.
Nakanishi, N., Renfer, E., Technau, U. and Rentzsch, F. (2012). Nervous systems of the sea anemone Nematostella vectensis are generated by ectoderm and endoderm and shaped by distinct mechanisms. *Development* **139**, 347-357.
Pilon, M. and Weisblat, D. A. (1997). A nanos homolog in leech. *Development* **124**, 1771-1780.
Plickert, G., Jacoby, V., Frank, U., Müller, W. A. and Mokady, O. (2006). Wnt signaling in hydroid development: formation of the primary body axis in embryogenesis and its subsequent patterning. *Dev. Biol.* **298**, 368-378.
Plickert, G., Frank, U. and Müller, W. A. (2012). *Hydractinia*, a pioneering model for stem cell biology and reprogramming somatic cells to pluripotency. *Int. J. Dev. Biol.* **56**, 519-534.
Putnam, N. H., Srivastava, M., Hellsten, U., Dirks, B., Chapman, J., Salamov, A., Terry, A., Shapiro, H., Lindquist, E., Kapitonov, V. V. et al. (2007). Sea anemone genome reveals ancestral eumetazoan gene repertoire and genomic organization. *Science* **317**, 86-94.
Schmitt-Engel, C., Cerny, A. C. and Schoppmeier, M. (2012). A dual role for nanos and pumilio in anterior and posterior blastodermal patterning of the short-germ beetle *Tribolium castaneum*. *Dev. Biol.* **364**, 224-235.
Shen, R. and Xie, T. (2010). NANOS: a germline stem cell's Guardian Angel. *J. Mol. Cell Biol.* **2**, 76-77.
Siemen, H., Colas, D., Heller, H. C., Brüstle, O. and Pera, R. A. (2011). Pumilio-2 function in the mouse nervous system. *PLoS ONE* **6**, e25932.
Soza-Ried, J., Hotz-Wagenblatt, A., Glatting, K. H., del Val, C., Fellenberg, K., Bode, H. R., Frank, U., Hoheisel, J. D. and Frohme, M. (2010). The transcriptome of the colonial marine hydroid *Hydractinia echinata*. *FEBS J.* **277**, 197-209.
Sugiyama, T. and Fujisawa, T. (1978). Genetic analysis of developmental mechanisms in *Hydra*. II. Isolation and characterization of an interstitial cell-deficient strain. *J. Cell Sci.* **29**, 35-52.
Szczepanek, S., Cikala, M. and David, C. N. (2002). Poly-gamma-glutamate synthesis during formation of nematocyst capsules in *Hydra*. *J. Cell Sci.* **115**, 745-751.
Teo, R., Möhrlen, F., Plickert, G., Müller, W. A. and Frank, U. (2006). An evolutionary conserved role of Wnt signaling in stem cell fate decision. *Dev. Biol.* **289**, 91-99.
Toledano, H., D'Alterio, C., Czech, B., Levine, E. and Jones, D. L. (2012). The let-7-Imp axis regulates ageing of the *Drosophila* testis stem-cell niche. *Nature* **485**, 605-610.
Torras, R. and González-Crespo, S. (2005). Posterior expression of nanos orthologs during embryonic and larval development of the anthozoan Nematostella vectensis. *Int. J. Dev. Biol.* **49**, 895-899.
Torras, R., Yanze, N., Schmid, V. and González-Crespo, S. (2004). nanos expression at the embryonic posterior pole and the medusa phase in the hydrozoan *Podocoryne carnea*. *Evol. Dev.* **6**, 362-371.
Vessey, J. P., Schoderboeck, L., Gingl, E., Luzi, E., Riefler, J., Di Leva, F., Karra, D., Thomas, S., Kiebler, M. A. and Macchi, P. (2010). Mammalian Pumilio 2 regulates dendrite morphogenesis and synaptic function. *Proc. Natl. Acad. Sci. USA* **107**, 3222-3227.
Wikramanayake, A. H., Hong, M., Lee, P. N., Pang, K., Byrum, C. A., Bince, J. M., Xu, R. and Martindale, M. Q. (2003). An ancient role for nuclear beta-catenin in the evolution of axial polarity and germ layer segregation. *Nature* **426**, 446-450.
Wu, H. R., Chen, Y. T., Su, Y. H., Luo, Y. J., Holland, L. Z. and Yu, J. K. (2011). Asymmetric localization of germline markers Vasa and Nanos during early development in the amphioxus Branchiostoma floridae. *Dev. Biol.* **353**, 147-159.
Ye, B., Petritsch, C., Clark, I. E., Gavis, E. R., Jan, L. Y. and Jan, Y. N. (2004). Nanos and Pumilio are essential for dendrite morphogenesis in *Drosophila* peripheral neurons. *Curr. Biol.* **14**, 314-321.

```
Hydractinia_Nanos2        -PLVHSNTPQVPPRSSTS-----LQVCVFCRNNG--------------ESESVYTSHVLK 40
Clytia_Nanos2             -PLPPS-QPQNRGASTNSNNNNGVQVCVFCRNNG--------------ESESVYTSHVLK 44
Hydra_cnnos2              -TLYNS-HDSLTLRASSN-------VCVFCRNNG--------------ESENVYASHVLK 37
Nematostella_nanos2       --LGKP-TARSSAPGANR------QVCVFCRNNG--------------ESEEVYASHVLK 37
Hydra_cnnos1              --QQQIQSKALKNLSKTS-------VCVFCRNNG--------------ESREFYSSHTLK 37
Hydractinia_Nanos1        --PPLSKDSRLSKANKTT-------VCVFCRNNG--------------ESKEFYSSHTLK 37
Clytia_Nanos1             --PFHSSHHNRKNAAKAT-------VCVFCRNNG--------------ESREFYSSHTLK 37
Nematostella_nanos1       -------NRENKKNRNAN-------VCVFCRNNG--------------ESKKVYSSHVLK 32
Ephydatia_nanos           ---TFSKLPTQQPIKKQQ-------VCVFCRNNG--------------ESESFYTSHYLK 36
Mus_nanos1                --------ARLLKPELQV--------CVFCRNNK--------------EAVALYTTHILK 30
Homo_nanos1               --------ARLLKPELQV--------CVFCRNNK--------------EAMALYTTHILK 30
Xenola_xcat2              -----------ESVGHKG--------CGFCRSNR---------------EALSLYTSHRLR 27
Homo_nanos3               ----------ESSPAPER-------LCSFCKHNG--------------ESRAIYQSHVLK 29
Mus_nanos3                ----------ESSAAPER-------LCSFCKHNG--------------ESRAIYQSHVLK 29
Danio_nanos               ---------PKSSPAERK-------FCSFCKHNG--------------ETEAVYTSHYLK 30
Homo_nanos2               ---------PGANGGLGT-------LCNFCKHNG--------------ESRHVYSSHQLK 30
Mus_nanos2                ---------EGYPGCLPT-------ICNFCKHNG--------------ESRHVYTSHQLK 30
Platynereis_nanos         LLLTITRSKHKAPTGKKN-------ICVFCKTNG--------------EGEVIYTSHVLK 39
Botryllus_nanos           ALLPSSPNARTQILPVAR-----FIGCSFCKNNK--------------EVKEWYMSHKLK 41
Dugesia_nanos             -LLHKVRTS-NQIRKESH-----IELCVFCRNNN--------------EPFEMYVSHKVK 39
Haliotis_nanos            --RGDVTQLQVQGKKKSK------LICVFCKNNK--------------EPPHVYTGHVLK 38
Helobdella_nanos          ----------GKSGEPAL-------VCVFCRNNK--------------EPECVANSHLVK 29
Drosophila_sim_nanos      -----YKRYN-SKAKEIS------RHCVFCENNN--------------EPEAVINSHSVR 34
Drosophila_nanos          -----YKRYN-SKAKEIS------RHCVFCENNN--------------EPEAVINSHSVR 34
Musca_nanos               -----QKRYNGPKNEKYSS----AKHCVFCENNN--------------EPDAVVKSHAVR 37
Chironomus_nanos          ---KKMDKKNSIKKKKMD------DHCVFCKNNG--------------ADEILYKSHTVK 37
Anopheles_nanos           ------KCRN-KSTCELD-------HCVFCFNNK--------------ADREVYESHRCK 32
Celegans_nanos1           --------PRGNPPHPLC--------CCFCFGTASEFARLHTLPAPRKDDRGPWSDHCSK 44
Celegans_nanos2           -------VPSLFKRREYG--------CGYCRSVG----------------YMRWETHTRK 29
                                                  * :*                        *  :

Hydractinia_Nanos2        DTEGRTACPILRAYT-CPICKANGDGSHTIKYCPLNQNTR-----------AGVMGQQP- 87
Clytia_Nanos2             DTDGRTSCPILRAYT-CPICKANGDNSHTIKYCPMNQNARMMGQNGNNQGNAGLFPRPPF 103
Hydra_cnnos2              DTDGRTSCPILRAYT-CPICKANGDNSHTIKYCPMNQNAR----------SASTFNGLS- 85
Nematostella_nanos2       SADGKTTCPILRAYT-CPICKASGDDSHTIKYCPQNQQTQ----------GNGQLPPPP- 85
Hydra_cnnos1              DNEGNTMCPILRAYT-CPLCKSHGNQSHTIKYCPKYTPKP----------KTDKLLGIS- 85
Hydractinia_Nanos1        DNEGNTTCPILRAYT-CPLCKANGDNSHTIKYCPKYTPKM----------KADKLLGIS- 85
Clytia_Nanos1             DSEGNTSCPILRAYT-CPLCKANGDSSHTVKYCPKYTPKV----------KAEKLLHLN- 85
Nematostella_nanos1       DAEGNTTCPILRAYT-CPLCKASGSQSHTIKYCPKNKNGS----------KLQAKV---- 77
Ephydatia_nanos           DAEGKVTCPVLRAYT-CPLCGANGDGAHTIKYCPENSQSV----------RNGGIGKRQ- 84
Mus_nanos1                GPDGRVLCPVLRRYT-CPLCGASGDNAHTIKYCPLSKVPPPTVRP-----PPRSNRDSLP 84
Homo_nanos1               GPDGRVLCPVLRRYT-CPLCGASGDNAHTIKYCPLSKVPPPPARP-----PPRSARDGPP 84
Xenola_xcat2              ALDGRVLCPVLRGYT-CPLCGANGDWAHTMRYCPLRRLLRD----------PQSNSNNP- 75
Homo_nanos3               DEAGRVLCPILRDYV-CPQCGATRERAHTRRFCPLTGQGYTS--------VYSHTTRNSA 80
Mus_nanos3                DEAGRVLCPILRDYV-CPQCGATQEHAHTRRFCPLTSQGYTS--------VYCYTTRNSA 80
Danio_nanos               NRDGDVMCPYLRQYK-CPLCGATGAKAHTKRFCPMVDKNYCS--------VYAKSTW--- 78
Homo_nanos2               TPDGVVVCPILRHYV-CPVCGATGDQAHTLKYCPLNGG-QQS--------LYRRSGRNSA 80
Mus_nanos2                TPEGVVVCPILRHYV-CPLCGATGDQAHTLKYCPLNSS-QQS--------LYRRSGRNSA 80
Platynereis_nanos         EKNGRVCCPILRAYK-CPNCGAHGDTAHTLKYCPLSVENQKR--------LRRPPFGIF- 89
Botryllus_nanos           NNAGKVTCPVLRCYE-CPLCEATGDNAHTIGHCPLNPNRHSS--------LPLAIRSKAN 92
Dugesia_nanos             DLNGKVTCPVLRNYT-CPLCNSTGDFAHTIKYCPISSNSSKS--------LVE------- 83
Haliotis_nanos            DSRGYTACPVLRKYP-CPICQAIGDHAHTIKYCPFNNDSEFR-------TSPSPLRTTRM 90
Helobdella_nanos          DEKGQVTCPILYIYT-CPICGATGKAAHTIKYCPYNTGERFYVPP-----LTRKTGNRSQ 83
Drosophila_sim_nanos      DNFNRVLCPKLRTYV-CPICGASGDSAHTIKYCPKKPIIT----------MEDAIKAESF 83
Drosophila_nanos          DNFNRVLCPKLRTYV-CPICGASGDSAHTIKYCPKKPIIT----------MEDAIKAESF 83
Musca_nanos               DSMGRVLCPKLRTYI-CPICKASGDKAHTVKYCPQKPIIT----------MEDAVNAESF 86
Chironomus_nanos          DLKGRVLCPKLRAYQ-CPICGADGDQSHTVKYCPKKPIVT----------MEDLKKLDAS 86
Anopheles_nanos           DEAGNVTCPVLQTFV-CMRCKATGTKAHTAKYCPLKPVIT----------PEDCLAME-- 79
Celegans_nanos1           K-RGRVVCPKLRSMV-CGICGATGDNAHTTKHHLEAFGDD-------------------- 82
Celegans_nanos2           K------CDKLSSLAPCKICGARGEMNHTETYCPMKPSSQLFFN----EDFSRDFENRRF 79
                                 *  *     *  * :     **  .
```

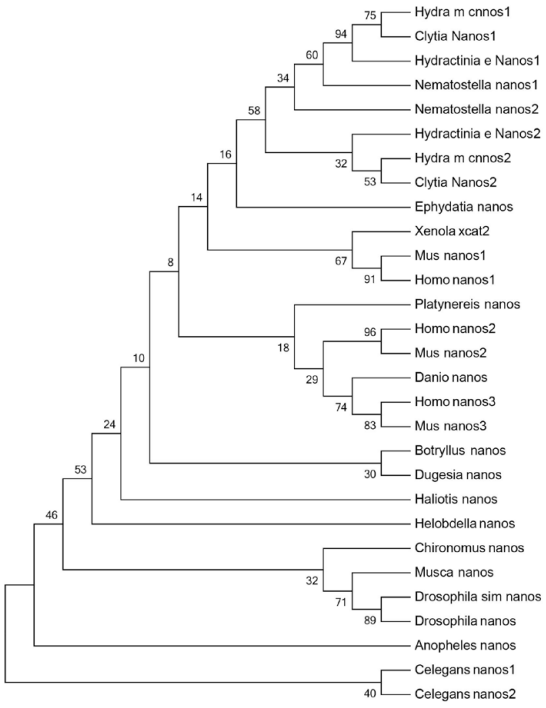

Fig. S1. Alignment of Nanos proteins from various animals and inferred phylogenetic tree. Bootstrap values are given.

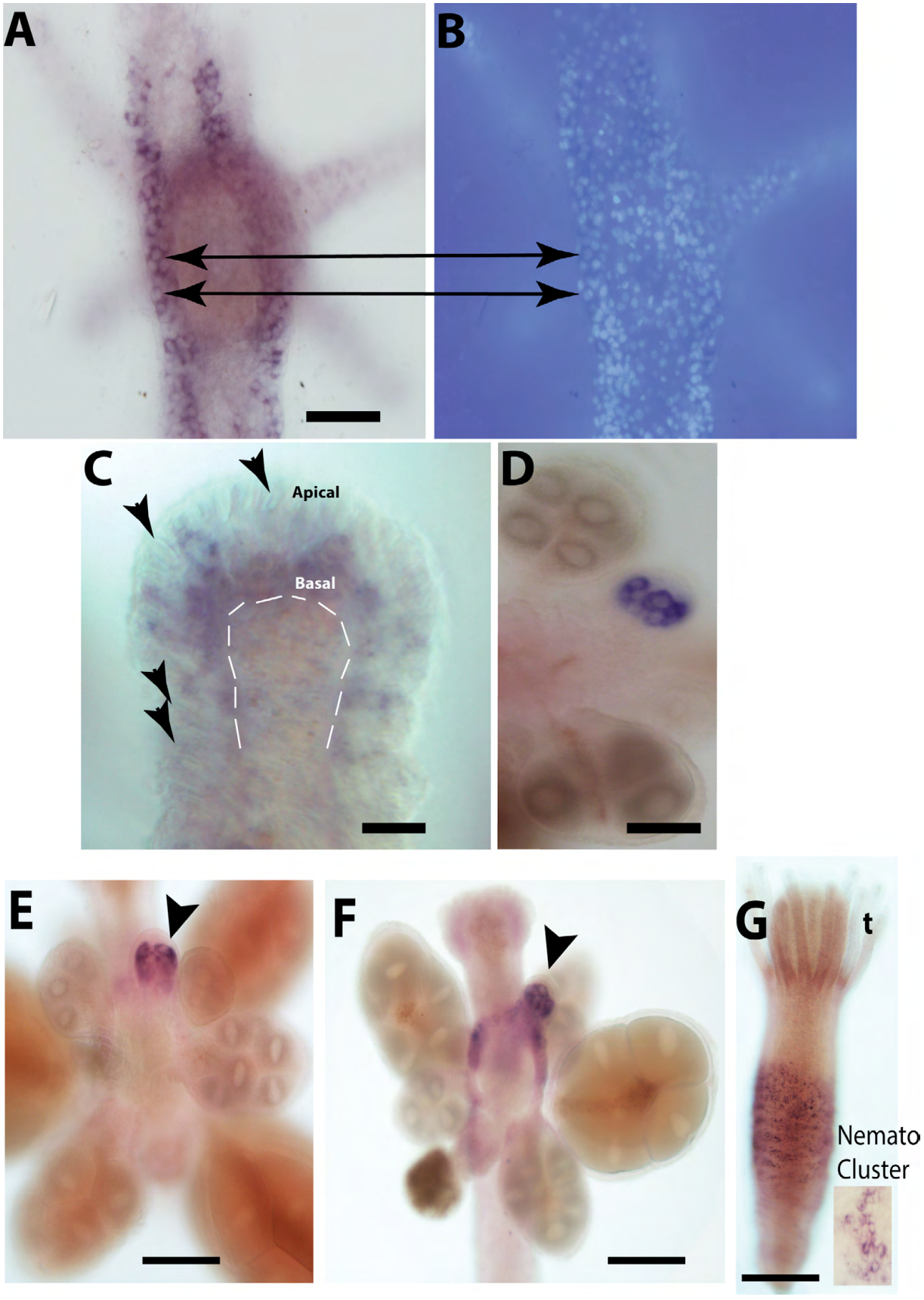

Fig. S2. *Nanos2, Nanos1* and *Pumilio* expression. (A-D) *Nanos2.* (A) Stolon of primary polyp, viewed from below; bright light. (B) The same animal as (A) but under UV light showing DAPI positive nuclei. Double headed arrows point to the same cells. (C) A tentacle. Mature nematocytes, apically mounted in battery cells and ready to discharge, are marked by arrows. *Nanos2*+ cells are only basally located. Dashed line represents the position of the mesoglea. (D) Sexual polyp. *Nanos2*+ developing oocytes are visible. (E) *Nanos1* expressing oocytes. (F) *Pumilio* expression in oocytes. (G) *Pumilio* expression in nematoblasts in a mature feeding polyp. Inset shows nematoblasts cluster. Scale bars 50 µm in (A); 10 µm in (C); 200 µm in (D-G).

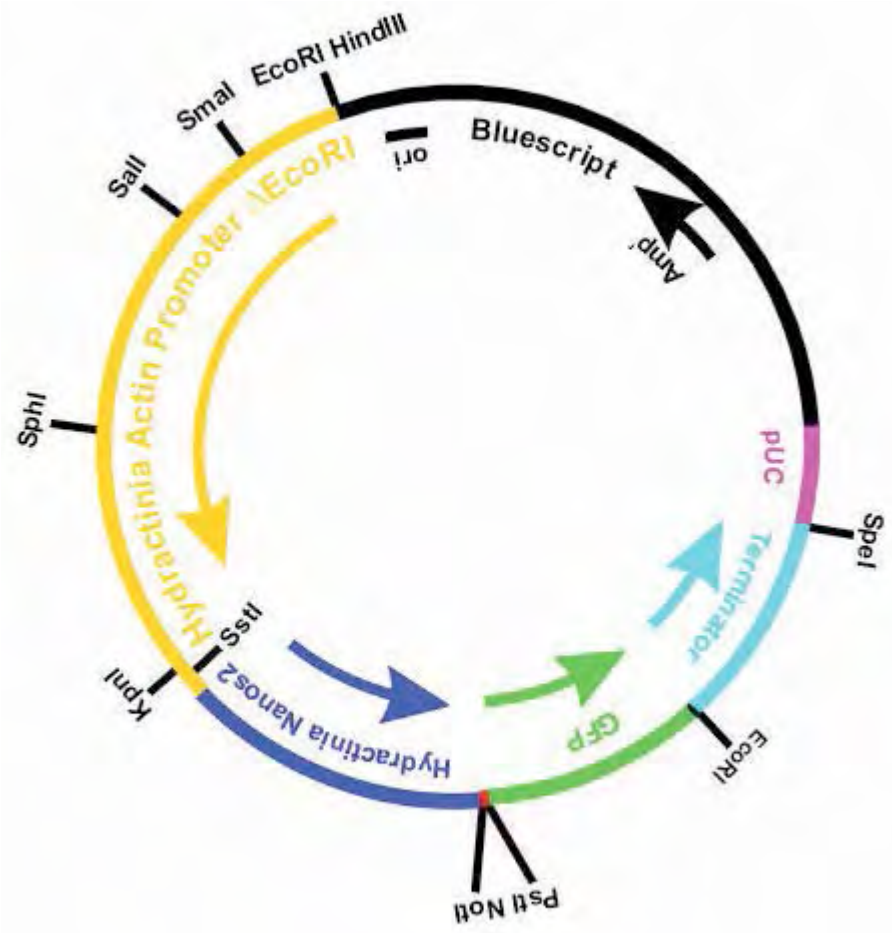

Fig. S3. Structure of the *Nanos2* ectopic expression construct.

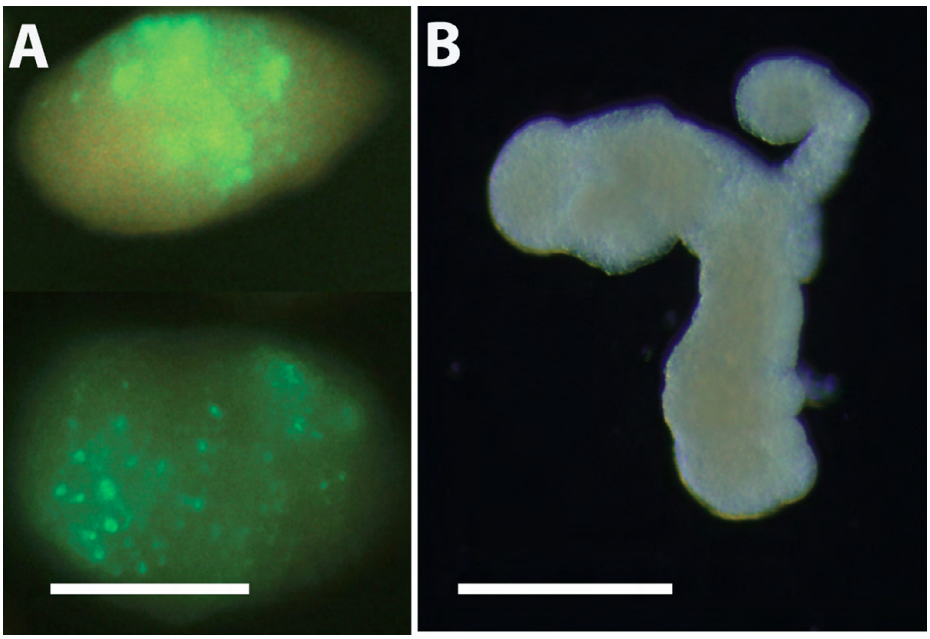

Fig. S4. (A) Transgenic, mosaic larvae expressing Nanos2-GFP. Scale bar represents 100 µm. (B) Aberrantly developed transgenic *Nanos2* embryo. Scale bars 100 µm.

Table S1. Oligonucleotides used during the study

Oligo name	Oligo sequence
Nanos1ATG-T7-fwd	gatcataatacgactcactatagggatgttcaaggcaatgtatagcaatgtt
Nanos1Sp6-rev	tagcaatttaggtgacactatagaaggtggttttgttggccttagacaat
Nanos2fwd-ATG	atgtcgttgagtgatgttatgcta
Nanos2revRNAi	aatcctgaaataaggaaaaatcacttgc
Nanos2fwdRNAiT7	ggatcctaatacgactcactatagggatgtcgttgagtgatgttatgc
Nanos2revRNAisp6	gatctaatttaggtgacactatagaaaatcctgaaataaggaaaaatc
Nanos2revpro1	tatgcggccgccatctttctttagaaattctttttttcaacaacaaa
Nanos2rev-TAA	catccttacctttccatgctggtt
Nanos2-RT-fwd2	acagcaaatcaacagccgaat
Nanos2-RT-rev2	gaaggcggttgtgcaggta
Nanos2promoterrev-NotI	tatgcggccgcctttctttagaaattctttttttcagcaac
Promoter_insertionUFPrev-FseI	aatggccggccactggccgtcgttttacaaca
Nonos2promoterfwd-FseI	taaggccggccttcctgtgttgttgcggtg
Splinkerout	cgaatcgtaaccgttcgtacgagaa
Splinkerin	tcgtacgagaatcgctgtcctctcc
Ash-T7-fwd	gatcataatacgactcactataggggcaccgattaacaaatgatgca
Ash-sp6-rev	tagcaatttaggtgacactatagaataacagcgaagaaatatttacaatcta
RFamide-T7fwd	gatcataatacgactcactatagggatgttaatcatggcttcaaaggc
RFamide-sp6rev	tagcaatttaggtgacactatagaacttaacagtctctactttcgtgttg
Ncol1-T7 fwd	gatcataatacgactcactatagggacgtccaggaccaccaggagta
Ncol1-Sp6 rev	tagcaatttaggtgacactatagaactgggcaacagtattgtggacaaga
Pumilionestrev1	ggtcctgttccagtagactgaagat
Pumilionestfwd1	aagcattggagactataccaccagaa
Pumilio ATG start fwd	atgcgcgacatcatttggcaacaa
Pumilio RACE rev1	ggattcttgccaatgattttcaaaagtaaacat
Pumilio stop-TGA-rev	aacttcttcaatcaacatagaacgttcagc
Pumilio rev3	catttacaataggaataccaccattttgacc
PumilioRACE rev2	ttgcgaacttgagtagttttatcccag
Pumiliorev4	atgaaaagagttggttcttctgattcat
Pumilio T7-fwd	gatcataatacgactcactatagggatcggaggtcatcttcagtctact
Pumilio sp6-rev	tagcaatttaggtgacactatagaatacatgtattgtcatttctggtggtat
T7 Promoter	taatacgactcactatagggg
Sp6 Promoter	atttaggtgacactatagaa
pGEM-T RNAi Fwd	ggcgctttctcatagctcac
pGEM-T RNAi Rev	taccgggttggactcaagac
pGEM-T RNAi fwd 2	cgacaggactataaagataccaggc
T7pGEM-T RNAi fwd2	atcctaatacgactcactatagggcgacaggactataaagataccaggc
GFP-TAGstop-rev	ctatttgtatagttcatccatgccat
Spliced leader	actcacactatttctaagtccctgag
Splice leader long	aacgcggggacagataaaaaaactcacactatttctaagtccctgagtttaag
Smart UPM long	ctaatacgactcactatagggcaagcagtggtatcaacgcagagt
Smart UPM short	ctaatacgactcactatagggc
Nanos2 morpholino	gcataacatcactcaacgacatctt
Control morpholino	cctcttacctcagttacaatttata